

# First Results from an Airborne Ka-band SAR using SweepSAR and Digital Beamforming

Gregory A. Sadowy, Jet Propulsion Laboratory / California Institute of Technology, USA  
Hirad Ghaemi, Jet Propulsion Laboratory / California Institute of Technology, USA  
Scott C. Hensley, Jet Propulsion Laboratory / California Institute of Technology, USA

## Abstract

SweepSAR is a wide-swath synthetic aperture radar technique that is being studied for application on the future Earth science radar missions. This paper describes the design of an airborne radar demonstration that simulates an 11-m L-band (1.2-1.3 GHz) reflector geometry at Ka-band (35.6 GHz) using a 40-cm reflector. The Ka-band SweepSAR Demonstration system was flown on the NASA DC-8 airborne laboratory and used to study engineering performance trades and array calibration for SweepSAR configurations. We present an instrument and experiment overview, instrument calibration and first results.

## 1 Introduction

### 1.1 Overview

This paper describes a demonstration of airborne synthetic aperture radar (SAR) using the SweepSAR measurement technique. This approach employs an array-fed reflector that illuminates a wide swath on transmit but uses digital beamforming (DBF) on receive to capture simultaneous subswaths. This combines the relative simplicity of a reflector antenna (as compared to a planar phased array) with the performance advantages of DBF SAR system. The SweepSAR approach is being studied for implementation on future Earth science radar missions.

Designs under study for future missions employ interferometric SAR (InSAR) systems operating at L-band (1.2-1.3 GHz) frequencies with reflectors in the 6-15m size range. The frequency choice is driven by radar phenomenology of the desired measurements and the antenna size is driven by radar SNR and ambiguity performance requirements.

In order demonstrate the SweepSAR technique and provide a technology test bed for SweepSAR hardware, an airborne demonstration has been developed. Since antennas of 6-m or greater are generally impractical for airborne operation, we reduced the size of the antenna by increasing the frequency but keeping the characteristic geometry used in L-band radar studies.

### 1.2 SweepSAR Technique

The advantages of the SweepSAR approach as compared to the wide range of other techniques that have been developed for wide-swath SAR are detailed in [1]. The antenna system is composed of a reflector fed by a linear array feed. This approach exploits the fact

that as the feed is displaced from the center, the peak of the radiation pattern shifts. Thus, each element of the feed array has a radiation pattern that peaks in a different direction. As feed point moves further from the focal axis, the beam begins to degrade. However, with the distances required by the SweepSAR approach (typically  $<20\lambda$ ) the beam performance remains acceptable for many applications.

The pattern of each feed point corresponds to a range of angles of arrival and also (ignoring topography) corresponds to a range of cross-track distances. Each of these corresponds to one subswath. By digitally combining the signals from multiple receive swaths, wider swaths can be generated.

In typical SweepSAR operation, all feed array elements transmit simultaneously, illuminating the entire swath sequentially by a short pulse. For sufficiently short pulses, only part of the receive feed array is receiving echoes at any given time. As the pulse travels from the near range to the far range of the swath, the received echo sweeps from one end of the feed array to the other. This can dramatically reduce the data compared to a planar beamformer (which must receive at every element all the time).

## 2 Demonstration System

### 2.1 System Description

Table 1 gives the important operating parameters of the SweepSAR Airborne Demonstration System. The system consists of the following main parts: 1) 16-channel array-fed reflector 2) waveguide transmit array 3) RF subsystem 4) digital receiver system and 5) Embedded GPS/INS (EGI). Unlike L-band spaceborne SweepSAR concepts that use the same array to transmit and receive, the airborne demonstration uses

a separate transmit array to generate the required fan beam. This approach was chosen because development of a 16-channel high-power transmit/receive array was not practical for this demonstration. Instead, an active receive-only feed was developed.

**Table 1.** Airborne SweepSAR Demo Parameters

Parameter	Value
Frequency	35.6 GHz
Bandwidth	80 MHz
Sampling Frequency	240 MHz
PRF	1300 Hz
Flight Altitude	8750-10500 m
Transmit Power	250W

## 2.2 Ka-band Array-fed Reflector

Figure 1 shows the 40-cm array-fed reflector system. The reflector was precision-machined from aluminum and contains features to enable laser metrology of the reflector location. The metrology data are used to determine the location of antenna with respect to the EGI center of navigation. The reflector and feed are held in place by a high-stability feed arm manufactured from Invar alloy. The feed arm is attached to a common plate with the EGI. A radome (not shown) protects the system from weather, dirt and debris.

The 16-element active array feed (Figure 1, inset) is a 16x2 element microstrip patch array fabricated on Rogers Duroid 6002. The back side of the board carries 16 low-noise amplifiers (LNAs) and a heater circuit to provide temperature stabilization of the feed. A calibration coupler fabricated on the front side of the feed allows calibration signals to be coupled into the feed array. Precise specification or manufacturing of the calibration coupler is not necessary. The coupling

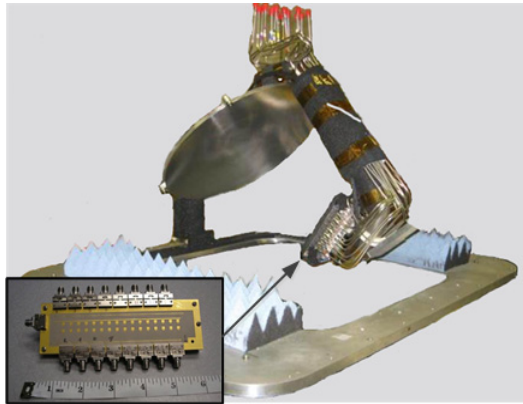


**Figure 1.** Reflector and feed on main structure. Inset shows 16-element active receive feed detail

coefficients are determined as part of the array calibration process.

## 2.2.1 Digital Receiver System

The digital receiver system was originally described in [2]. Up to sixteen signals from the receive antenna system are downconverted to L-band and fed into an array of L-band digital receivers which sample at a rate of 240 MS/s. Data from all channels are packed together and multiplexed into a high-speed serial data stream which is then carried over a fiber-optic cable to the Data Acquisition Controller (DAC). The DAC embeds precise timing and header information and writes the data stream to a disk array for storage. Since this is an experimental system for demonstrating DBF techniques and calibration, no real-time beamforming is performed. Performing beamforming in post-processing permits assessment of the effectiveness of different calibration and beamforming approaches. However, due to the high output data rate from the digital receiver array, a spaceborne system would likely require real-time digital beamforming.

## 3 Airborne Experiment

### 3.1 Aircraft Integration

Figure 2 shows the location of the SweepSAR Demonstration hardware in the Nadir-2 port of the NASA DC-8 Airborne Laboratory. The receive antenna is contained in a recessed box in the cargo bay of the aircraft. The receive antenna looks at a 30 degree angle through a rectangular aperture containing the radome. The EGI is also mounted in the pressure box, on the same plate that carries the receive antenna. The transmitter antenna (a slotted-waveguide array) is mounted on an external plate. In addition to providing a clear view for the transmit antenna, this arrangement minimizes coupling between the transmit and receive antennas. The recessed box forms the pressure interface. The inside (containing the receive antenna) is at ambient pressure. On top of the pressure box (inside the pressurized cargo bay of the DC-8) is an electronics plate carrying the RF downconverters, digital receivers and serial-link interface. During this initial demonstration, eight digital receiver channels were used.

### 3.1 Experimental Setup

In order to establish system performance it was desirable to collect data over targets with known characteristics. We achieved this by placing trihedral corner reflectors on a dry lake bed in the Mojave desert (inset, Figure 6). The lake bed provides the darkest background available and the corner reflectors allow us to evaluate the system point target response.



**Figure 2.** Installation in NASA DC-8: (a) Feed (b) reflector (c) transmit array. Radome has been removed for photo.

The eight receiver channels used in this experiment covered an angular range of 35-40 degrees from nadir, corresponding to a swath of approximately 1.4 km at our operating altitudes of 8750-10500 m AGL. Two flights were conducted over the test site and adjacent areas of interest. Multiple passes were collected over each site in order to assess calibration and beamforming stability over time

## 4 Results

### 4.1 Antenna Calibration

Prior to installation in the aircraft, the antenna system was calibrated on a near-field scanner. All antennas and the radome were integrated into the DC-8 pressure box and oriented such that direction corresponding to nadir in the aircraft installation is perpendicular to the scanner plane.

The calibration measurement has two parts. The first is a conventional near-field measurement of each receive element pattern and the transmit array pattern. These patterns are recorded for later use in the beamforming algorithm.

The second part of the calibration procedure measures the amplitude and phase of the calibration couplers that are built into the feed. Figure 4 shows that calibration setup. A high-speed switch is used to switch the range excitation signal rapidly back and forth between the scanner probe and the antenna calibration port. This switch operates continuously during the entire near-field scan, synchronous with the scanner data collection. A small error (<10 degrees) may be introduced by phase change due to flexure in the cable (marked HG in diagram) but this can largely be removed by taking the average value over the scan.

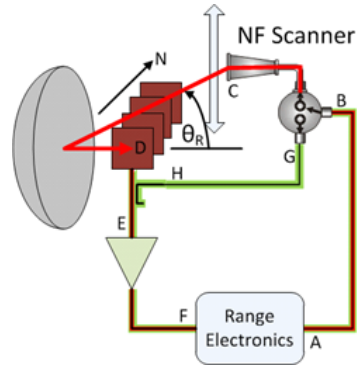
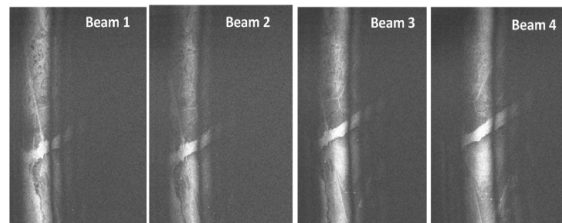


**Figure 4.** Near-field calibration of antenna. (a) Photo of antenna system on scanner. (b) Calibration diagram

During airborne operations, a calibration signal is injected into the same calibration port on the antenna. The beamforming processor extracts and filters this calibration signal. The beamforming processor then uses timing and aircraft attitude data from the EGI to map echo time into the corresponding angle in the radiation pattern data. Finally, the near-field range calibration measurements, measured radiation patterns and airborne calibration measurements are combined to in order to generate the proper complex coefficients for beamforming.

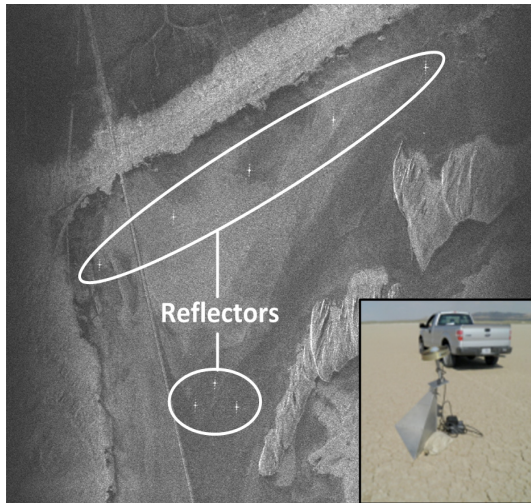
### 4.2 Imaging Performance

In order to establish a performance baseline, each receiver's data was processed in into strip maps using SAR processing without beamforming. Figure 5 shows strip maps from the first four receiver channels. Note that the main beam and close-in sidelobe are visible in the image. Each successive beam has a subswath that is further in range than the previous one.



**Figure 5.** SAR images from first four individual beams

After establishing baseline performance, the raw data was processing using the near-field and airborne calibration data to perform conjugate field match (CFM) beamforming. After calibration and beamforming, images were formed using the same SAR processor as the images in Figure 5. The digital beamforming and calibration process runs independently of SAR image generation, prior to SAR processing.



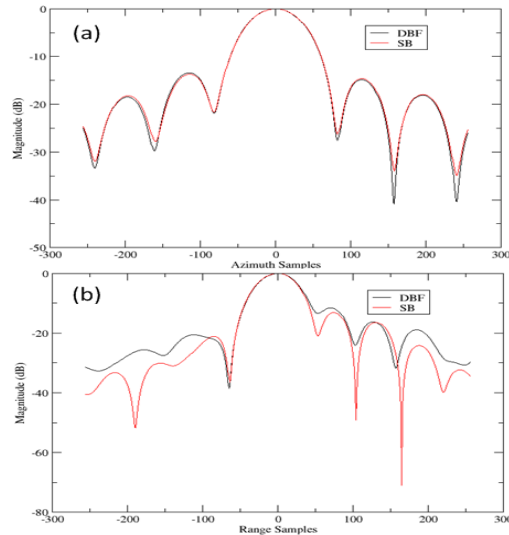
**Figure 6** Beamformed image of calibration site. Inset: Photo of corner reflector on lake bed

Figure 6 is a digitally-beamformed image of the lakebed calibration site. Eight corner reflectors are visible in the image. The beamformed image shows good radiometric continuity across the swath. There are no visible artifacts from the individual receiver antenna patterns (some of which had poor sidelobe suppression, as can be seen in Figure 5).

The corner reflectors show up as bright point targets, achieving the expected resolution in range and azimuth. Figure 7 shows azimuth and range cuts through a corner reflector for both the beamformed and non-beamformed cases. For the azimuth cut, the point target responses are almost identical. This is not surprising since the beamforming primarily affects the range direction. The corner reflector cut in range shows that the resolution of the beamformed case is identical to that of the non-beamformed case. However, the sidelobe levels differ slightly below approximately -20 dB with the sidelobes of the DBF images being slightly higher. This may be due to errors measurement calibration coefficients and receive element patterns. In most applications, this performance would be acceptable.

### 3 Conclusions

We have described the development and operation of a Ka-band airborne demonstration of the SweepSAR measurement technique using an array-fed reflector. Notwithstanding the difficulties of making accurate phase calibration measurements at this short wavelength, we have demonstrated successful collection of airborne-data and generation of digitally-beamformed SAR imagery of comparable quality to single receiver imagery, except with eight times wider swath. This Ka-band demonstration will serve as a technology



**Figure 7.** Cuts through corner reflector

testbed for the development of techniques and hardware for future Earth science radar missions.

### Acknowledgements

The authors would like to thank Ernie Chuang, Roger Chao, Brandon Heavey, Eric Liao, Sean Lin, Timothy Miller, Dragana Perkovic, Momin Quddus, Mauricio Sanchez-Barbety, Scott Shaffer, Jordan Tanabe and Tushar Thrivikraman for help in design, assembly, test and operation of the SweepSAR Demo system. This work was performed at the Jet Propulsion Laboratory / California Institute of Technology under contract with the National Aeronautics and Space Administration.

### References

- [1] Freeman, A.; Krieger, G.; Rosen, P.; Younis, M.; Johnson, W.; Huber, S.; Jordan, R.; Moreira, A., "SweepSAR: Beam-forming on receive using a reflector-phased array feed combination for spaceborne SAR," *Radar Conference, 2009 IEEE*, vol., no., pp.1-9, 4-8 May 2009
- [2] Sadowy, Gregory; Ghaemi, Hiran; Heavey, Brandon; Perkovic, Dragana; Zawadzki, Mark; Moller, Delwyn; , "Ka-band Digital Beamforming and SweepSAR Demonstration for Ice and Solid Earth Topography," *Synthetic Aperture Radar (EUSAR), 2010 8th European Conference on*, vol., no., pp.1-4, 7-10 June 2010